

Observation of a bias-dependent constrained magnetic wall in a Ni point contactKoji Sekiguchi,^{*} Akinobu Yamaguchi, and Hideki Miyajima
*Department of Physics, Keio University, Hiyoshi 3-14-1, Yokohama 223-8522, Japan*Atsufumi Hirohata
*Department of Electronics, University of York, Heslington, York, YO10 5DD, United Kingdom*Shinji Usui
Cybernet Systems Co., Ltd., Kanda-Neribeicho 3, Chiyoda, Tokyo 101-0022, Japan
(Received 5 August 2008; revised manuscript received 16 September 2008; published 22 December 2008)

Quantized electron transport in a Ni point contact exhibits nonlinear bias dependence without an external magnetic-field application. The nonlinear features are categorized into two distinctive types dependent on the shapes, which are confirmed based on our measurements on hundreds of break junctions. Such nonlinear characteristics are unique to a magnetic point contact, showing the contribution of spin-dependent transport within a microscopic magnetic structure. *Ab initio* calculations on atomic wire model demonstrate that the magnetic point contact is comprised of an abrupt change in magnetic moments at the contact region, drastically modifying only the flow of a spin-down current. The calculations reproduce the nonlinear features observed experimentally. Our results therefore offer a method to analyze the spin transport in a magnetic point contact without a magnetic-field application, which can minimize the ambiguity in the origin of ballistic magnetoresistance [Phys. Rev. Lett. **83**, 2425 (1999)].

DOI: [10.1103/PhysRevB.78.224418](https://doi.org/10.1103/PhysRevB.78.224418)

PACS number(s): 75.47.De, 72.25.Ba, 75.47.Jn, 75.60.Ch

Quantum effects at room temperature have been intensively investigated in metallic nanostructures.¹ For instance, the conductance quantization of integer multiples of $2e^2/h$ ($\equiv G_0$) has been experimentally observed in nanoconstrictions, where a chain of atoms, called a point contact (PC), is fabricated by pulling off both ends of two bulk electrodes across the contact.^{2,3} When the PC is prepared with ferromagnetic metals, such as Fe, Ni and Co, electron spins give rise to the peculiar quantization of integer multiples of e^2/h ($\equiv G_0/2$), where the factor of 2 corresponds to the spin degeneracy and is spontaneously lifted in the ferromagnets.^{4,5} In addition, when a magnetic structure of such a magnetic point contact (MPC) is rearranged by the application of an external magnetic field, the MPC offers giant magnetoresistance (MR) [or ballistic magnetoresistance (BMR)],⁶ which is induced by the modulation of spin-dependent quantum transport across the MPC.

To date, the intrinsic origin of such spin-dependent quantum phenomena has been considered to be due to a magnetic domain wall (DW) trapped in the MPC.⁷ Prominent theoretical studies have predicted that the DW width in the MPC is constrained and, hence, holds an abrupt change in the magnetization direction.⁸ The exchange coupling among the magnetic moments in the constrained DW is, therefore, very different from the well-known Néel and Bloch walls, in which the magnetic moments gradually rotate their orientation in order to minimize the total energy.⁹ Although several experimental groups have attempted to explain their observed BMR in the MPC by assuming the existence of such a constrained DW, they have only qualitatively dealt with the transport process in the quantum channel.^{6,10} In addition, the existence of BMR itself has been challenged since some experimental studies have revealed that a large resistance change in the MPC may be induced by extrinsic effects, such as the magnetostriction.¹¹⁻¹³ Even for a carefully designed

system,¹⁰ these extrinsic effects cannot be excluded because of the application of an external magnetic field. The experimental proof of the constrained wall in the absence of an external magnetic field is, therefore, essential to confirm the appearance of BMR.

The purpose of this paper is to inquire the possibility of the formation of a constrained DW within a MPC fabricated by a break-junction method.^{4-6,13-15} Our experimental results of current-voltage (I - V) characteristics in the quantized states clearly demonstrate that two distinct types of nonlinear transport are induced in the MPC without an external magnetic-field application. *Ab initio* calculations further reveal that the nonlinear I - V characteristics dominantly originate from a spin-down current in combination with the magnetization configurations between the two electrodes.

A MPC was fabricated by the break-junction method with using a Ni wire (0.1 mm in diameter) and a Ni thin film (150 nm in thickness).^{13,14} Both the wire and film electrodes were mounted in a vacuum chamber to make the first contact at 4.2 K, which allowed us to sustain a MPC stably in the time scale of a few seconds. Under a bias of 250 mV across the electric circuit, the conductance quantization was first measured as shown in Fig. 1(a). Once a stable conductance plateau was obtained, I - V measurement was carried out by applying a slowly changing bias voltage with a triangular wave form, of which peak-to-peak amplitude was 500 mV. In our experiment, the I - V curves were found to be reproducible under the same MPC configurations. The electrodes were finally separated after the I - V measurement was completed and were contacted again to repeat the above measurement steps.

Figures 1(b) and 1(c) represent the I - V characteristics observed in the different MPC with the quantized conductance G_0 , showing two distinct types of nonlinearity. In the lower bias region $|V| < 50$ mV, both I - V curves presented follow

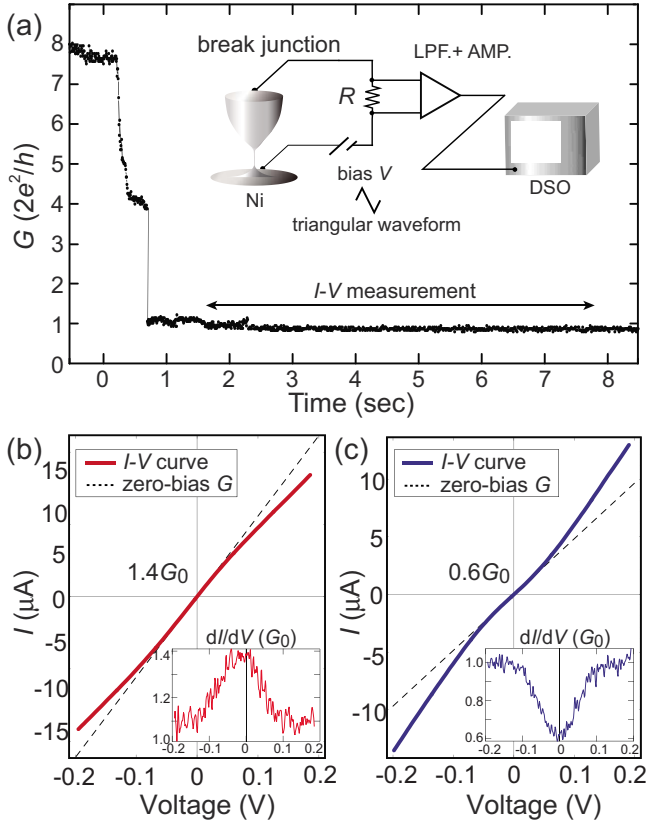


FIG. 1. (Color online) (a) Conductance quantization for a ferromagnetic Ni point contact. Panels (b) and (c) represent two distinct I - V curves, which deviate downward and upward from the zero-bias G ($dI/dV_{V=0}$, broken lines), respectively. Each nonlinearity is characterized by the differential conductance (dI/dV), revealing nonequilibrium transport.

the corresponding zero-bias conductances (G) of $1.4G_0$ and $0.6G_0$. With increasing bias voltage, however, the I - V curves deviate either [Fig. 1(b)] downward or [Fig. 1(c)] upward from the zero-bias G . The ratios between downward and upward I - V curves are experimentally found to be 20% and 70% of the total curves, respectively. The rest of 10% shows linear characteristics. Each nonlinearity is clearly distinguished by calculating the differential conductance (dI/dV) as shown in the inset of each panel. For the higher bias $|V| > 200$ mV, each differential conductance approaches G_0 , of which conductance plateau (nonequilibrium) is different from those appeared in the vicinity of $V=0$ (equilibrium), indicating the quantum-transport channel is modified by the finite bias-voltage application. It should be noted that these nonlinearities have experimentally vanished (i.e., linear) when $G > 14G_0$, clearly indicating that the presence of the quantum channel is essential for the nonlinear transport. This critical conductance value corresponds to the MPC cross-sectional diameter of 1.1 nm estimated by using the Sharvin formula.¹⁶

In our experiments, a nonmagnetic PC does not exhibit such nonlinearities under the identical experimental condition. The I - V characteristics for the nonmagnetic PC made of Cu, Pb and Au always show linear dependence on the bias voltage (Fig. 2), unambiguously proving that the observed

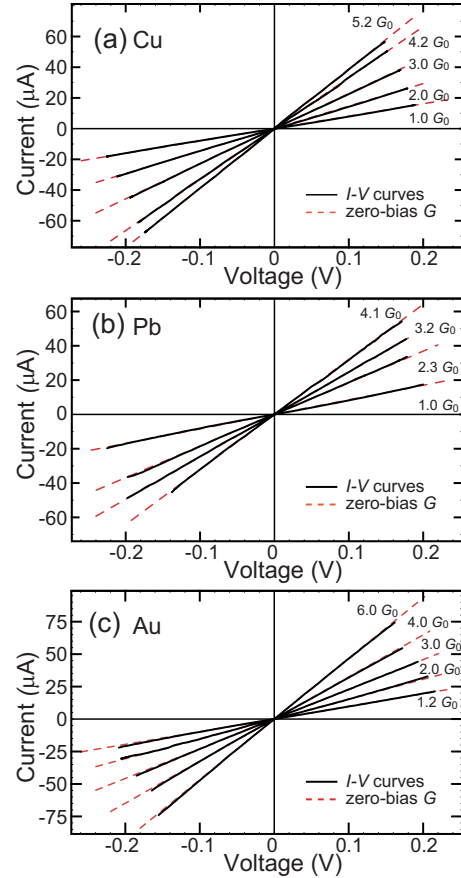


FIG. 2. (Color online) Representative I - V characteristics of nonmagnetic point contacts measured at the quantized plateaus at a finite bias voltage.

nonlinearities in the Ni MPC are of magnetic origin, and are different from the nonlinear I - V characteristics as previously reported.²

Experimentally, the conductance difference $\Delta G \equiv |G_{V=200 \text{ mV}} - G_{V=0}|$ is not constant even when the MPC possesses the same conductance, meaning that the quantum electron transport within the MPC strongly depends on the magnetic structures of the individual MPC. In order to understand the geometry dependence, the ΔG is collected from all the measured I - V curves, whose $dI/dV_{V=0}$ are below $5G_0$, within which the area of the PC (0.67 nm in diameter) can be treated as the quantum channel according to the Sharvin formula.¹⁶ Figure 3 shows the distribution of ΔG for both the Ni and Cu PC. The ΔG distribution for Ni is apparently much broader ranging from $0.01G_0$ to $0.5G_0$ and is fitted very well with the chi-square (χ^2) distribution with five degrees of freedom ($n=5$), which means that five independent variables contribute to the conductance difference: ΔG can be expressed by the sum of squares as $\Delta G = g \sum_{i=1}^5 (t_i)^2$, using variables t_i and an arbitrary constant g . This shows an analogy to the Landauer-Büttiker framework. This fit also suggests that the conductance difference is provided by five independent transmission channels, corresponding to the number of the spin-down channels consisting of five ($3d$) orbitals. This indicates random interaction patterns, such as complicated spin-dependent scattering and nonuniform spin-

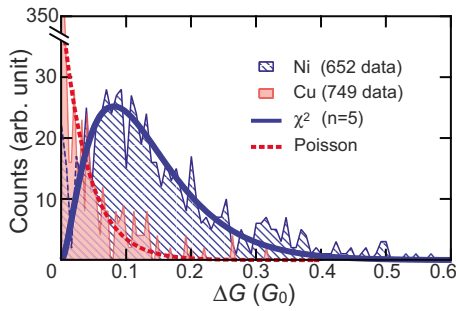


FIG. 3. (Color online) The slashed histogram represents the statistical distribution of ΔG for the ferromagnetic Ni PC, while the shaded one denotes that for nonmagnetic Cu. The χ^2 -distribution function for Ni is given by $P(\Delta G) = a(b\Delta G)^{3/2} \exp(-b\Delta G/2)$, where a and b are fitting parameters ($a=1786$ and $b=18.87 \pm 0.7$). The Poisson distribution for Cu is given by $P(\Delta G) = a\lambda^{b\Delta G} \exp(-\lambda)/(b\Delta G)!$, where λ is the average value of $\Delta G (=0.066)$ and a and b are fitting parameters ($a=40$ and $b=4.34$).

wave density within the MPC, resulting in the broader distribution of ΔG . Possible contribution from a d orbital has also been suggested for the case of nonmagnetic Pt contact,¹⁷ which may also be applicable to our cases.

On the other hand, the distribution for Cu is narrower and centered at $\Delta G=0$, which is well-fitted by the Poisson distribution function, confirming the linear I - V curves measured. The distinction in the distributions between the MPC and the nonmagnetic PC strongly indicates the presence of spin-polarized transport in association with the magnetic structures in the MPC.

In order to further investigate the origin of the nonlinear I - V behaviors, *ab initio* calculations are carried out on the spin-dependent transport in the MPC by using ATOMISTIX TOOLKIT 2.2.¹⁸ This program is based on the density-functional theory and a nonequilibrium Green's-function method¹⁹ and takes spins of electron explicitly into account in its self-consistent calculations of an electronic density of states. A one-dimensional (monatomic) Ni wire is modeled as a MPC,²⁰ of which magnetic moments are allowed to precess their directions and to change their magnitude to minimize the total energy to represent a collinear MPC structure, while those of the left and right electrodes are fixed to form either parallel or antiparallel configuration.

Figure 4 represents calculated I - V curves for the Ni MPC. Schematic illustration in each panel represents atomic and magnetic configuration. In Fig. 4(a), the magnetizations of the electrodes (boxed atoms) are set to align in parallel. The I - V curve exhibits downward convex from the zero-bias G for $V>0$, quantitatively reproducing our experimental finding displayed in Fig. 1(b) with the same threshold values for both the bias voltage and the current. As shown in the inset, the spin-resolved I - V curves demonstrate that a spin-up current increases linearly with increasing bias voltage, while a spin-down current shows a peak at $V=1.0$ V. Corresponding transmission spectra of the spin-down electrons are exhibited in the bottom panel of Fig. 4(a), showing that the transmission spectrum at the equilibrium ($V=0$) is comprised of six transmission channels, i.e., one ($4s$) and five ($3d$) orbitals, and is monotonically suppressed with increasing bias voltage across the electrodes.²¹

On the other hand, a calculated I - V curve for the antipar-

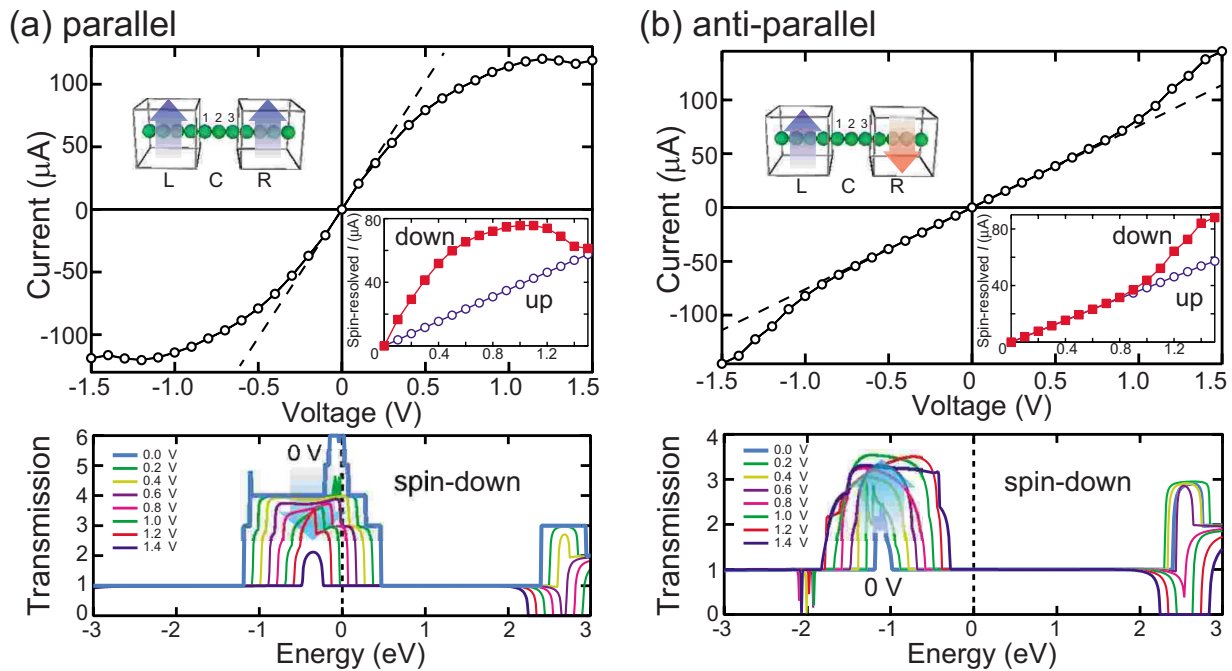


FIG. 4. (Color online) *Ab initio* calculations for a one-dimensional Ni MPC for the cases of both (a) parallel and (b) antiparallel magnetization configurations. The schematic illustrations represent calculation models, which are divided into three regions: a left electrode (L), a magnetic point contact (C), and a right electrode (R). Top panels show the calculated I - V characteristics and zero-bias conductance $dI/dV_{V=0}$ (broken lines). Insets exhibit spin-resolved I - V characteristics, showing significant contributions of the spin-down electrons. Bottom panels depict the evolution of the transmission spectrum for the spin-down channel. Here, the Fermi energy E_F at the equilibrium is set to be zero.

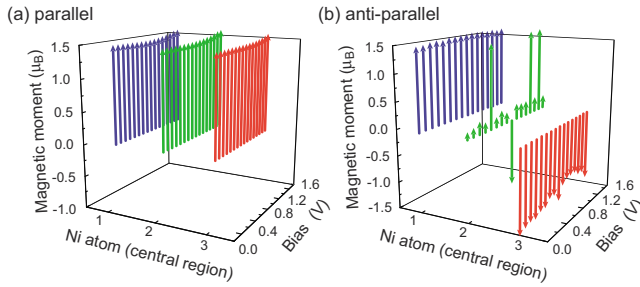


FIG. 5. (Color online) Magnetic moments in the three Ni atoms in the MPC for the cases of both (a) parallel and (b) antiparallel magnetization configurations with respect to the bias voltage across the electrodes. The magnetic moment of the i th Ni atom is defined as $M_i \equiv q_{i\uparrow} - q_{i\downarrow}$, where $q_{i\uparrow}$ and $q_{i\downarrow}$ are spin-up and spin-down Mulliken populations of the i th Ni atom, respectively.

allel magnetization configuration deviates upward from the zero-bias G again due to the spin-down current [see Fig. 4(b)], reproducing the experiment in Fig. 1(c). As shown in the bottom figure of Fig. 4(b), the transmission of the spin-down electrons consists of a single channel at the equilibrium and is gradually enhanced with increasing the magnitude of the bias voltage. Therefore, in both parallel and antiparallel configurations, the spin-down currents are revealed to play a critical role for the nonlinearity. In the antiparallel case, however, the threshold voltage, where the deviation starts, is calculated to be larger (800 mV) than the experimental results (50 mV). This departure may be attributed to the fact that our calculation model is oversimplified as discussed below.

The magnetic moments within the MPC (Ni atoms labeled $i=1, 2$ and 3) are calculated as depicted in Fig. 5. Note that the magnitude of the magnetic moment cannot be determined *a priori* but is resolved as a result of a finite bias (nonequilibrium transport) since the electron (spin) density is determined by the flow of electrons from the electrodes. For the parallel configuration [Fig. 5(a)], all the magnetic moments in the MPC are almost identical, showing gradual minor variations with increasing bias voltage. The exchange interaction among the electron spins is considered to be the same for the parallel configuration, and hence, the MPC does not disturb both up and down spin flows. For the antiparallel configuration [Fig. 5(b)], the magnetic moments of both Ni1 and Ni3 are also calculated to be aligned along those of their neighboring electrodes. The magnetic moments at the equilibrium ($V=0$) are found to be $1.44\mu_B$ and $-1.43\mu_B$ for Ni1 and Ni3, respectively. Remarkably, the magnetic moment of Ni2 is found to be $0.059\mu_B$, meaning that our calculation reproduces a softening of a magnetic moment as have similarly reported in theoretical prominent works.^{22,23} The softening is a significant proof of the existence of a constrained DW, and thus, the transition MPC region comprised of these three Ni atoms represents a constrained DW very well. Our calculations further demonstrate that the softening of the magnetic moment is valid even for the nonequilibrium state. Interestingly, such moment softening also vanishes at certain nonequilibrium states, such as at $V=0.4$ V, where the magnetic moments are $1.46\mu_B$, $1.46\mu_B$ and $-1.3\mu_B$ for Ni1, Ni2 and Ni3, respectively, but maintaining an abrupt change in the moments, i.e., a constrained DW.

The presence of such a constrained DW induces BMR in combination with the bias voltage. A total current for the antiparallel configuration can exceed that for the parallel configuration when $V > 1.2$ V, meaning that an inverse sign of magnetoresistance can experimentally be observed. For instance, the magnetoresistance ($MR = G_P/G_{AP} - 1$, where G_P and G_{AP} are the conductances for the parallel and antiparallel configurations, respectively) is approximately 140% when $V=200$ mV, while MR is -25% when $V=1.5$ V, which have been similarly measured by García *et al.*²⁴ Our *ab initio* study clearly shows the bias dependence of the constrained DW under the absence of a magnetic field, agreeing with both positive and negative BMRs observed experimentally, which provides further insight into the origin of the BMR.

The actual structure of the MPC is not ideal, implying that the magnetic moments of the MPC do not perfectly follow the parallel or antiparallel configurations of the electrodes. Because of the three dimensionality of the electrodes, the magnetic moments of the electrodes can possess a mutual angle (noncollinear),^{22,23} which is stochastically induced by the break-junction method and gradually reduces the exchange energy in a certain distance as occurs in the Bloch and Néel walls in a larger scale.⁹ The mutual angle is an additional parameter which tunes the threshold bias, where the deviation starts in the nonlinear I - V curves but does not change the global features in the I - V characteristics. Besides, we need to consider the possibility of an antiferromagnetic coupling induced by Ni chain oxidation. The antiferromagnetic coupling between the Ni chain and the electrodes introduces spin-dependent channels in the MPC, which is different from our calculation model and leads to change in the threshold bias. Even so, it should be noted that our observed nonlinearities do not follow the expected electron-transport behaviors through a Ni-O tunnel barrier. The 20% of nonlinearities [Fig. 1(b)] are different from a typical tunneling I - V curve and the 70% of nonlinearities [Fig. 1(c)] show linear dependence in $|V| < 50$ mV, suggesting that the dominant transport mechanism is Ohmic through the Ni metallic chain. Therefore, the nonlinearities should be attributed to the magnetic configuration (constrained DW) in the MPC.²⁶

In conclusion, I - V characteristics of a MPC are measured without a magnetic-field application, revealing two distinct types of nonlinearities, which reflect microscopic magnetic configurations in the MPC. *Ab initio* calculations quantitatively support the experimental findings and further imply that a spin-down current predominantly controls the nonlinearity with respect to both the magnetic configurations of the bulk regions and the bias voltage. In addition, the detailed *ab initio* simulations for the MPC demonstrate that a constrained domain wall can be formed in the MPC and significantly disturbs the flow of a spin-down current at certain bias voltages, providing both positive and negative BMR.

We acknowledge Atomistix A/S for supporting the calculation of our *ab initio* simulations. This work was partly supported by Grants-in-Aid for Scientific Research on Priority Areas from the Ministry of Education, Culture, Sports, Science and Technology, Japan.

*koji@ssc1.kuicr.kyoto-u.ac.jp

- ¹N. Agrait, A. L. Yeyati, and J. M. van Ruitenbeek, Phys. Rep. **377**, 81 (2003).
- ²J. L. Costa-Krämer, N. García, P. García-Mochales, P. A. Serena, M. I. Marqués, and A. Correia, Phys. Rev. B **55**, 5416 (1997).
- ³H. Ohnishi, Y. Kondo, and K. Takayanagi, Nature (London) **395**, 780 (1998).
- ⁴T. Ono, Y. Ooka, and H. Miyajima, Appl. Phys. Lett. **75**, 1622 (1999).
- ⁵V. Rodrigues, J. Bettini, P. C. Silva, and D. Ugarte, Phys. Rev. Lett. **91**, 096801 (2003).
- ⁶N. García, M. Muñoz, and Y. W. Zhao, Phys. Rev. Lett. **82**, 2923 (1999).
- ⁷G. Tataru, Y. W. Zhao, M. Muñoz, and N. García, Phys. Rev. Lett. **83**, 2030 (1999).
- ⁸P. Bruno, Phys. Rev. Lett. **83**, 2425 (1999).
- ⁹S. Chikazumi, *Physics of Ferromagnetism* (Clarendon, Oxford, 1997).
- ¹⁰H. D. Chopra, M. R. Sullivan, J. N. Armstrong, and S. Z. Hua, Nature Mater. **4**, 832 (2005).
- ¹¹W. F. Egelhoff, Jr., L. Gan, H. Ettetgui, Y. Kadmon, C. J. Powell, P. J. Chen, A. J. Shapiro, R. D. McMichael, J. J. Mallet, T. P. Moffat, M. D. Stiles, and E. B. Svedberg, J. Appl. Phys. **95**, 7554 (2004).
- ¹²M. Gabureac, M. Viret, F. Ott, and C. Fermon, Phys. Rev. B **69**, 100401(R) (2004).
- ¹³K. Sekiguchi, E. Saitoh, and H. Miyajima, J. Appl. Phys. **97**, 10B312 (2005).
- ¹⁴K. Sekiguchi, M. Shimizu, E. Saitoh, and H. Miyajima, J. Magn. Mater. **282**, 143 (2004).
- ¹⁵J. M. van Ruitenbeek, A. Alvarez, I. Piñeyro, C. Grahmann, P. Joyez, M. H. Devoret, D. Esteve, and C. Urbina, Rev. Sci. Instrum. **67**, 108 (1996).
- ¹⁶Y. V. Sharvin, Sov. Phys. JETP **21**, 655 (1965).
- ¹⁷S. K. Nielsen, M. Brandbyge, K. Hansen, K. Stokbro, J. M. van Ruitenbeek, and F. Besenbacher, Phys. Rev. Lett. **89**, 066804 (2002).
- ¹⁸ATOMISTIX toolkit is available from QuantumWise A/S. See <http://www.quantumwise.com>
- ¹⁹M. Brandbyge, J. L. Mozos, P. Ordejón, J. Taylor, and K. Stokbro, Phys. Rev. B **65**, 165401 (2002).
- ²⁰Both the left and right electrodes contain four Ni atoms with infinite periodic boundary conditions of the unit cell ($a=b=c=9.12$ Å), while the MPC holds three Ni atoms. The Ni-Ni distance (2.28 Å) are set for the MPC in order to make the system energetically stable and to maintain net magnetic moments. Here, the Ni-Ni distance is defined to be slightly larger than a bulk lattice constant of 1.76 Å, which reflects the fact that the distance between the atoms in the PC is elongated as observed in Ref. 3. Spin-polarized generalized gradient approximation of Perdew, Burke and Ernzerhof (SGGA-PBE) is utilized as the exchange-correlation function, and double-zeta plus polarization (DZP) is applied as a basis set. Our model is simple but enough to reproduce our experimental results since the metallic point contact is revealed to be an atomic-scaled system (Ref. 5).
- ²¹A spin-up channel is comprised of a single transmission channel and unchanged for all the bias voltage calculated.
- ²²J. D. Burton, R. F. Sabirianov, S. S. Jaswal, E. Y. Tsybal, and O. N. Mryasov, Phys. Rev. Lett. **97**, 077204 (2006).
- ²³M. Czerner, B. Y. Yavorsky, and I. Mertig, Phys. Rev. B **77**, 104411 (2008).
- ²⁴N. García, H. Rohrer, I. G. Saveliev, and Y. W. Zhao, Phys. Rev. Lett. **85**, 3053 (2000).
- ²⁵A. R. Rocha, T. Archer, and S. Sanvito, Phys. Rev. B **76**, 054435 (2007).
- ²⁶The difference in the threshold bias may hold a key to understand the origin of the extremely large BMR as similarly suggested in Ref. 25 and needs to be systematically investigated.